# The Fredenhagen-Marcu operator in the gauge-Higgs Z(2) LGT at finite temperature

### B. Allés<sup>1</sup>

INFN Sezione di Pisa, Largo Pontecorvo 3, 56127 Pisa, Italy

### O. Borisenko<sup>2</sup>

INFN Gruppo Collegato di Cosenza, Arcavacata di Rende, 87036 Cosenza, Italy

N.N. Bogolyubov Institute for Theoretical Physics, National Academy of Sciences of Ukraine, 03143 Kyiv, Ukraine

### V. Chelnokov<sup>3</sup>

Institut für Theoretische Physik, Goethe-Universität Frankfurt, 60438 Frankfurt am Main, Germany

### A. Papa<sup>4</sup>

Dipartimento di Fisica, Università della Calabria

INFN Gruppo Collegato di Cosenza, Arcavacata di Rende, 87036 Cosenza, Italy

#### Abstract

We explore the possibility to use the Fredenhagen-Marcu operator as an order parameter of the deconfinement phase transition in gauge-matter systems at finite temperature. Concretely, we compute by numerical simulations this operator in the (2+1)-dimensional Z(2) lattice gauge theory (LGT) with Z(2)gauge fields coupled to Z(2)-valued Higgs fields. Our conclusion is that the Fredenhagen-Marcu operator can indeed serve as an order parameter capable of distinguishing the deconfinement phase from the Higgs and confinement phases of the theory.

<sup>1</sup>email: alles@pi.infn.it

 $^2$ email: oleg@bitp.kyiv.ua

<sup>3</sup>email: chelnokov@itp.uni-frankfurt.de

<sup>4</sup>email: papa@fis.unical.it

### 1 Introduction

Distinguishing the deconfined phase from the rest of the phase diagram in gauge theories with dynamical matter fields at finite temperature remains one of the important unsolved problems in high-energy physics. This problem appears especially relevant in the high-temperature region of QCD, where the deconfined phase is associated with the quark-gluon plasma phase. While the problem was solved long ago for the pure gauge theory by utilizing a gauge-invariant order parameter, the Polyakov (or temporal Wilson) loop, to distinguish the deconfined phase from the confined one, the situation gets much more complicated when dynamical matter fields in the fundamental representation are added to the action. Such fields explicitly break the global center symmetry of the theory and the Polyakov loop ceases to be a good order parameter.

Two operators able to differentiate between deconfined and other phases at zero temperature were constructed in the past. One is the Preskill-Krauss operator, designed for both Abelian and non-Abelian models with a non-trivial discrete center [1]. Its possible finite-temperature extension was proposed in [2, 3]. A difficulty with this operator is that, due to its highly non-local nature, it is hard to evaluate it numerically even in Abelian LGTs and there is no analytic tool to calculate the operator in non-Abelian models at small values of the gauge coupling constant, where the appearance of the deconfined phase is expected. The second operator is the Fredenhagen-Marcu (FM) operator proposed in [4]. It measures the ratio of two free energies: the free energy of a staple-like Wilson line squared and the free energy of the Wilson loop of double size in the temporal direction (the precise definition is given below). In the limit in which the sizes of the Wilson line and Wilson loop tend to infinity, this ratio is expected to vanish in the deconfined phase, while it approaches non-zero constant values in the confinement and other phases. Thus, the FM operator can test the presence of charged states in the vacuum. So far, this operator has been studied mainly in gauge-Higgs LGTs at zero temperature. Rigorous results confirming the expected behavior have been obtained for 4d U(1) [5] and Z(2) [6] gauge-Higgs systems. Numerical studies of the FM operator at zero temperature have been performed in Refs. [7, 8] for Z(2) models and in [9] for the SU(2) model. All results agree with analytic predictions. In a recent paper [10] we attempted the computation of the FM operator in the finite temperature SU(2)LGT. The results obtained suggest that, in the above-described large size limit, the FM operator might vanish in the deconfined phase of the theory. However, due to large statistical errors we could not state whether or not this is indeed the case. To get such unambiguous answer we have decided to study the (2+1)-dimensional

Z(2)-invariant gauge-Higgs model, whose relative simplicity allows to simulate it on larger lattices with bigger statistics. This is the aim of the present paper.

The partition function of the model on  $\Lambda \in \mathbb{Z}^{2+1}$  is defined as

$$Z_{\Lambda}(\beta, \gamma) = \sum_{\{z_n(x) = \pm 1\}} \sum_{\{s(x) = \pm 1\}} e^{S_G + S_H},$$
 (1)

where  $z_n(x)$  are the gauge fields and s(x) the Higgs fields. The gauge  $S_G$  and the Higgs  $S_H$  actions are given by

$$S_G = \beta \sum_{x} \sum_{n < m} z_n(x) z_m(x + e_n) z_n(x + e_m) z_m(x) ,$$
 (2)

$$S_H = \gamma \sum_{x} \sum_{n} s(x) z_n(x) s(x + e_n) . \tag{3}$$

Here,  $x = (x_1, x_2, t)$ , with  $t \in [0, N_t - 1]$ ,  $x_i \in [0, L - 1]$ , i = 1, 2, denotes a site on the lattice  $\Lambda$ . Using the notation  $l \equiv (x, n)$  for the link pointing in the direction n from the site x, we shall also employ the equivalent notation  $z(l) \equiv z_n(x)$ . On the other hand,  $x + e_n$  is the site beside x towards the direction n.

Periodic boundary conditions are imposed in all directions. The model is invariant under local  $Z_{\rm l}(2)$  transformations  $\omega(x)$  and global  $Z_{\rm gl}(2)$  transformation  $\alpha$ :

$$z_n(x) \rightarrow z'_n(x) = \omega(x)z_n(x)\omega(x+e_n)$$
, (4)

$$s(x) \rightarrow s'(x) = \omega(x)s(x)\alpha$$
 (5)

Thus, the full symmetry group is  $Z_1(2) \times Z_{gl}(2)$ . This model is self-dual in that, up to a constant, the partition function on the dual lattice maintains the form shown in Eq.(1) upon replacing the couplings  $\beta$ ,  $\gamma$  for their dual couplings  $\beta_d$ ,  $\gamma_d$  according to the relations

$$\gamma \to \gamma_d = -\frac{1}{2} \ln \tanh \beta , \qquad \beta \to \beta_d = -\frac{1}{2} \ln \tanh \gamma .$$
 (6)

This paper is organized as follows. In Sec. 2 we define the FM operator and discuss some simple analytic arguments to justify why we expect that its large size limit vanishes in the deconfined phase. Sec. 3 describes our numerical results and in Sec. 4 we present our conclusions.

# 2 The FM operator

The authors in [4] define the FM operator as follows. Let  $\mathcal{C}$  be a closed rectangular loop of size  $T \times R$ , with T and R the lengths along respectively the temporal and one spatial direction. We denote by  $W(\mathcal{C})$  the corresponding Wilson loop,

$$W(\mathcal{C}) = \prod_{l \in \mathcal{C}} z(l) . \tag{7}$$

By cutting  $W(\mathcal{C})$  into two halves along the temporal sides, we obtain a  $\sqcap$ - and a  $\sqcup$ -shaped objects. Let us take one of them, for instance  $\sqcap$ , and call it  $\mathcal{L}_{xy}$ , where x, y are the end points. Hence, the horizontal side of  $\sqcap$  is R lattice spacings long in the spatial direction, while the vertical sides run along the temporal direction and have lengths T/2. We then consider a gauge-invariant Wilson line, denoted by  $V(\mathcal{L}_{xy})$ , and obtained by multiplying  $\mathcal{L}_{xy}$  with the Higgs fields at the end points,

$$V(\mathcal{L}_{xy}) = s(x) \left( \prod_{l \in \mathcal{L}_{xy}} z(l) \right) s(y) . \tag{8}$$

The FM operator  $\rho$  is defined as the value of the ratio

$$H(R,T) = \frac{\langle V(\mathcal{L}_{xy}) \rangle^2}{\langle W(\mathcal{C}) \rangle} , \qquad (9)$$

in the large distance limit, viz.

$$\rho \equiv \lim_{R \to \infty} H(R, T) \ . \tag{10}$$

However, we will often simplify the language by employing "FM operator" to refer also to the ratio (9) itself.

Note that the above definition differs from the conventional one where one usually takes T = R before the limit in (10), so that in the limit  $R \to \infty$  both temporal and spatial sizes of the Wilson loop and line diverge. At finite temperature the size T cannot exceed the temporal lattice extent  $N_t$ , which is less than the spatial size L. The operator obtained by setting T to a constant value will be referred to as temporal FM operator. In the present work we compute both the temporal and the spatial FM operators. The latter is defined by taking spatial Wilson loops and spatial Wilson lines in Eq.(9) and imposing the standard constraint T = R.

It is not obvious that the large distance limit of the temporal FM operator vanishes in the deconfined phase if only R goes to infinity while T remains fixed. In

Ref. [10] we discussed simple non-rigorous arguments which prove why this can be the case in the SU(2) gauge-Higgs theory at finite temperature. Below we briefly outline those arguments for the Z(2) theory. It is also possible to prove rigorously that the large R limit of any FM operator vanishes in the deconfined phase of the Z(2) theory, if T is fixed and the limit is taken as in (10) [11].

Consider the region of small Higgs coupling  $\gamma \ll 1$ . Here the system can be in two phases, confined or deconfined, depending on the value of the gauge coupling. In the confined phase, corresponding to small  $\beta$ , the Wilson loop in the pure gauge theory decays with the area law  $\langle W(\mathcal{C})\rangle_G \approx (\tanh\beta)^{RT}$  and the leading perimeter law contribution comes from the Higgs action. Instead, for the Wilson line one gets

$$\langle V(\mathcal{L}_{xy}) \rangle = (\tanh \gamma)^{R+T} \left[ 1 + (2R + 2T - 2) \tanh^2 \gamma \tanh \beta + \cdots \right] + \sum_{\mathcal{M}_{xy}} (\tanh \gamma)^{|\mathcal{M}_{xy}|} \langle W(\mathcal{L}_{xy} \cup \mathcal{M}_{xy}) \rangle_G,$$
(11)

where the sum runs over all paths  $\mathcal{M}_{xy}$  connecting points x and y, while the Wilson loop  $W(\mathcal{L}_{xy} \cup \mathcal{M}_{xy})$  is constructed by closing the end points of  $\mathcal{L}_{xy}$  with the path  $\mathcal{M}_{xy}$ . The suffix G in  $\langle \cdots \rangle_G$  indicates that the expectation value is extracted in the pure gauge theory. Then, for any FM operator we find

$$H(R,T) \approx \frac{\left( (\tanh \gamma)^{R+T} + \dots + (\tanh \gamma)^R \left( \tanh \beta \right)^{\frac{RT}{2}} + \dots \right)^2}{(\tanh \gamma)^{2R+2T} + \dots + (\tanh \beta)^{RT} + \dots} . \tag{12}$$

The ratio goes to a constant in the limit  $R \to \infty$ , if T is fixed to a value larger than 2.

In the region of large  $\beta$  both temporal and spatial Wilson loops in the pure gauge theory decay with the perimeter law  $\langle W(\mathcal{C}) \rangle_G \approx \exp(-m(\beta)P(\mathcal{C}))$ . One gets

$$\langle W(\mathcal{C}) \rangle = \exp\left(-m(\beta)(2R+2T)\right) + (\tanh \gamma)^{2R+2T} , \qquad (13)$$

$$\langle V(\mathcal{L}_{xy})\rangle = (\tanh \gamma)^{R+T} + \sum_{\mathcal{M}_{xy}} (\tanh \gamma)^{|\mathcal{M}_{xy}|} \exp(-m(\beta)(R+T+|\mathcal{M}_{xy}|))$$
, (14)

where the constant  $m(\beta) \sim \mathcal{O}(e^{-\beta})$ . The leading contribution comes from the term  $|\mathcal{M}_{xy}| = R$  and gives

$$H(R,T) \approx (\tanh \gamma)^{2R} \frac{\left( (\tanh \gamma)^T + e^{-m(\beta)(2R+T)} \right)^2}{(\tanh \gamma)^{2R+2T} + e^{-m(\beta)(2R+2T)}}$$
 (15)

There is a competition between the two terms in the denominator: the first term arises due to screening from the matter fields, while the second term arises from the gluonic screening. If  $\beta$  is sufficiently large, the gluonic screening wins and we obtain

$$H(R,T) \approx \left(\tanh \gamma \ e^{m(\beta)}\right)^{2R+2T}$$
 (16)

Even if T is fixed,  $H(R,T) \to 0$  in the limit  $R \to \infty$ .

# 3 Numerical results

The phase diagram and universality class. The phase structure of the Z(2) gauge-Higgs LGT is well known both at zero and finite temperatures [12]. It includes three phases: confinement, deconfinement, and Higgs. The confinement phase at small gauge and Higgs couplings is separated from the Higgs phase at large  $\gamma$  by a smooth transition where the free energy and its derivatives remain analytic functions, in agreement with [13, 14]. This transition can, however, be described in analogy to spin-glass models by using an appropriate generalization of the overlap operator, see Ref [15] for a review of this approach. Such overlap operator was computed numerically for the Z(2) model at zero temperature in [8].

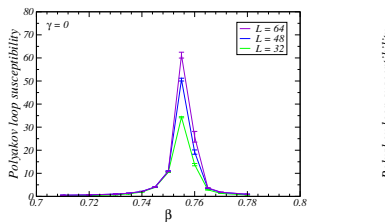
The deconfinement phase is separated from the confinement and Higgs phases by two lines representing thermodynamic transitions, which are in the 3d Ising universality class. These two lines merge in a multicritical point and continue as one line of first order phase transitions for a short interval. The end point of this first order transition is again in the Ising universality class.

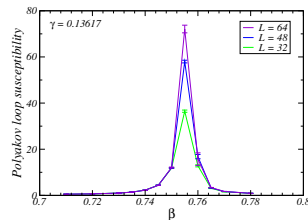
The phase structure just described is expected to stay essentially the same at finite temperature. The general phase diagram can be established by computing the Polyakov loop susceptibility. In Fig.1 we show this quantity in the vicinity of the confinement-deconfinement phase transition. Here, we fix the Higgs coupling and compute the Polyakov loop at various values of  $\beta$  on a lattice with temporal extent  $N_t = 16$  and several lattice spatial sizes L = 32, 48, 64. The peak of the susceptibility is clearly seen and grows with the lattice spatial size indicating a thermodynamic transition. To determine the precise location of the peak we employ multihistogram reweighting [16] to obtain the dependence of the susceptibility  $\chi$  on  $\beta$  in the vicinity of the simulated points. For each spatial size L, the peak position  $\beta_{\rm pc}(L)$  is identified from the condition  $\frac{\partial \chi}{\partial \beta} = 0$ . These pseudocritical couplings are then extrapolated to the thermodynamic limit using the finite-size scaling relation

$$\beta_{\rm pc}(L) = \beta_{\rm c} - AL^{-\frac{1}{\nu}} . \tag{17}$$

Once  $\beta_c$  is known, we can test universality by plotting the rescaled Polyakov loop susceptibility  $\chi L^{\eta-2}$  as a function of the rescaled coupling  $(\beta-\beta_c)L^{\frac{1}{\nu}}$ . Fig.2 shows this scaling collapse using the 2d Ising critical exponents  $\nu=1,\ \eta=1/4$ . The collapse is good except for a narrow region near the peak for the smallest lattice size (L=32), suggesting that the transition belongs to the 2d Ising universality class. For comparison, we repeated the same analysis using the 3d Ising critical exponents  $\nu\approx 0.6299709,\ \eta\approx 0.036297612$ , with the result shown in Fig.3. In this case the collapse fails both for the peak height, and width. In this way we locate the (vertical) critical line between confinement and deconfinement phases. The (horizontal) critical line between deconfinement and Higgs phases can be calculated from the duality relations (6).

The left panel of Fig.4 shows the Polyakov loop histogram for  $\gamma = 0.235$ . The two-peak structure indicates a first order transition. Finally, the right plot of Fig.4 presents the susceptibility in the crossover region, for  $\gamma > 0.240$ . One observes that the peak of the susceptibility does not grow with the lattice volume. The resulting phase diagram for  $N_t = 16$  is shown in Fig.5.





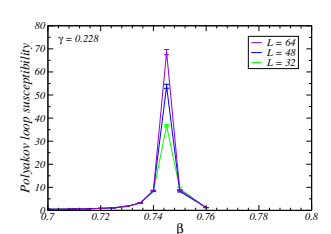


Figure 1: The Polyakov loop susceptibility as a function of  $\beta$  at fixed values of  $\gamma$  in the region of the second order phase transition for several spatial sizes.

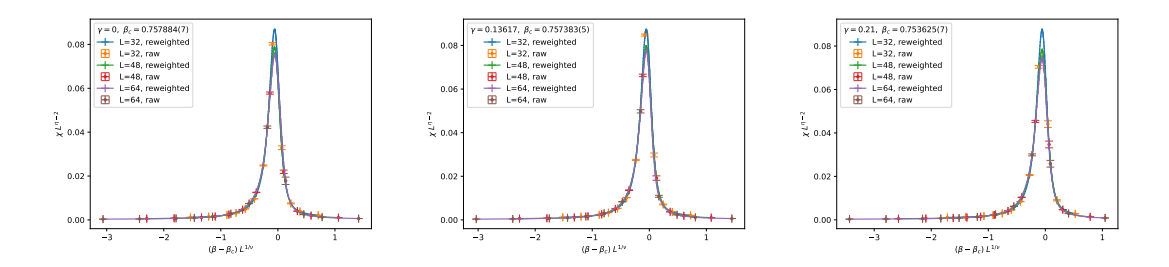


Figure 2: Collapse of the Polyakov loop susceptibility. Critical indices are fixed to the values in 2d Ising model:  $\eta=0.25$  and  $\nu=1$ . "Raw" data refers to the points obtained directly from Monte-Carlo simulations, while "reweighted" data are obtained using the multihistogram reweighting of raw data to intermediate values of gauge coupling  $\beta$ .

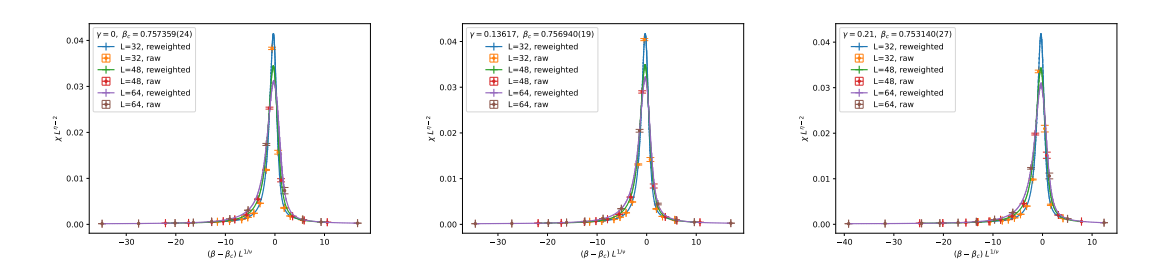
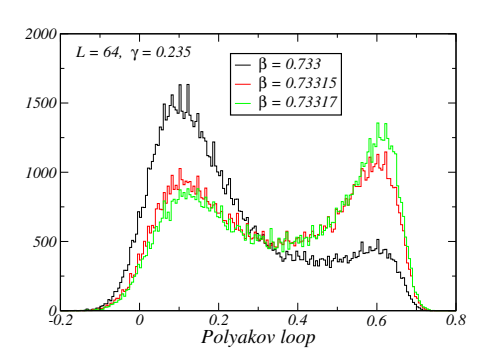


Figure 3: Collapse of the Polyakov loop susceptibility. Critical indices are fixed to the values in 3d Ising model:  $\eta \approx 0.03629$  and  $\nu \approx 0.63$ . The meanings of the labels are the same as in Fig.2.



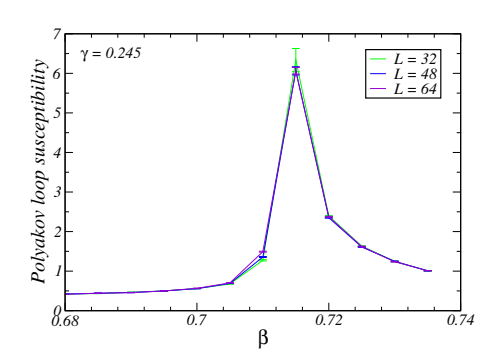


Figure 4: Left: Histogram of the Polyakov loop in the region of the first order phase transition. Right: The Polyakov loop susceptibility in the crossover region.

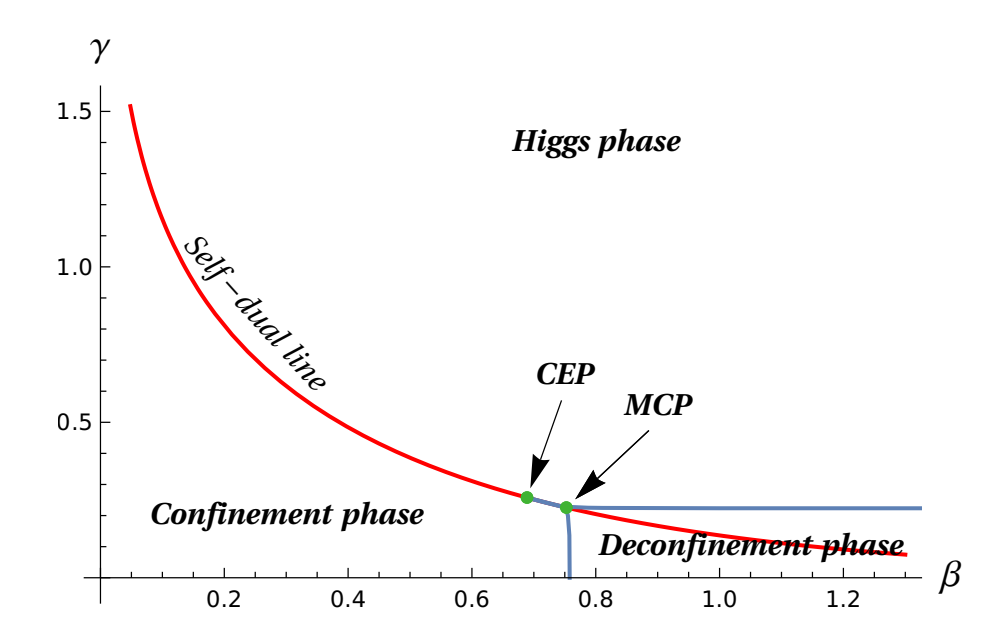
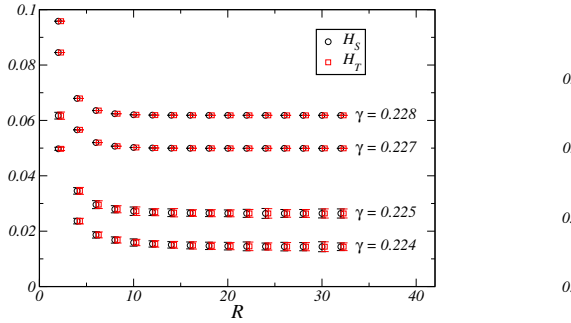


Figure 5: Phase diagram of the Z(2) gauge-Higgs theory on the lattice at finite temperature for  $N_t = 16$ . The acronym CEP stands for "critical end point" and MCP for "multicritical point". For other details see text.

The FM operator. We have computed the FM operator on lattices with temporal extent  $N_t = 16$  and spatial sizes L = 32, 48, 64, 96. The number of measurements varied between 100k and 400k per parameter set. To study the FM operator across

the deconfinement-Higgs phase transition we simulated the model at  $\beta=1.0$  and several  $\gamma$  values close to the critical point  $\gamma_c=0.2235$ . The behavior of the FM operator in the vicinity of the confinement-deconfinement transition was studied at  $\gamma=0.21$  and several gauge couplings close to the critical point  $\beta_c=0.7536$ . In all plots below we use the notations  $H_S$  and  $H_T$  respectively for the spatial and temporal FM operators. For the temporal operator we always use  $T=N_t/2$  in our simulations.



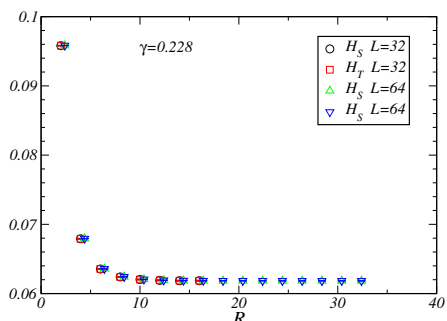
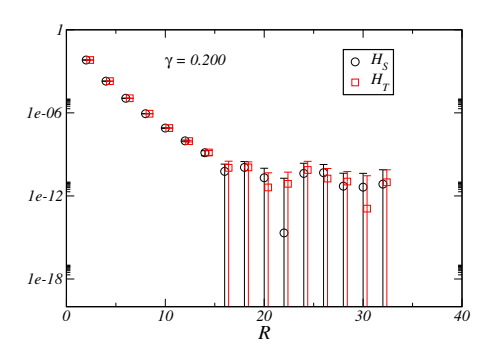


Figure 6: Left panel: the FM operators in the Higgs phase above the deconfinement transition for  $\beta=1$  and several  $\gamma$  values on a spatial size L=64. Data for  $H_T$  has been slightly shifted with respect to data for  $H_S$  for clarity purposes. Right panel: the FM operator for  $\beta=1$  and  $\gamma=0.228$  on two spatial sizes. Data for L=64 slightly shifted with respect to data for L=32 for clarity purposes.



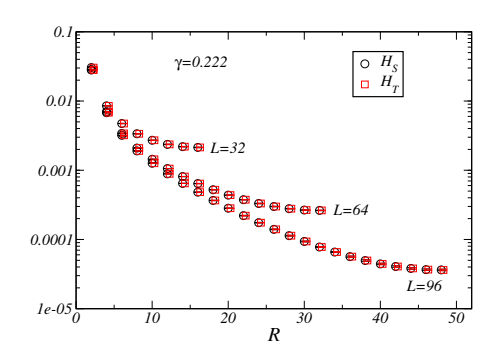
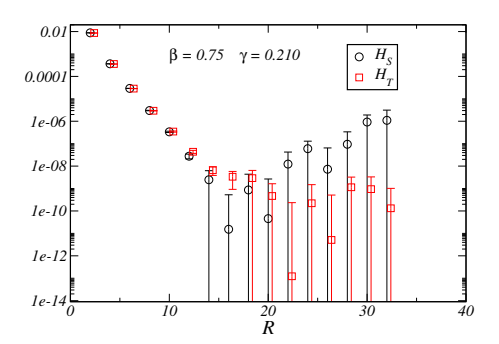


Figure 7: Left panel: the FM operator deeply in the deconfined phase on the lattice for  $\beta = 1$  with the spatial size L = 64. Right panel: the FM operator in the deconfined phase for  $\beta = 1$  close to the critical point on three spatial sizes. In both panels, data for  $H_T$  has been slightly shifted with respect to data for  $H_S$  for clarity purposes, and a logarithmic scale has been used for the vertical axis.



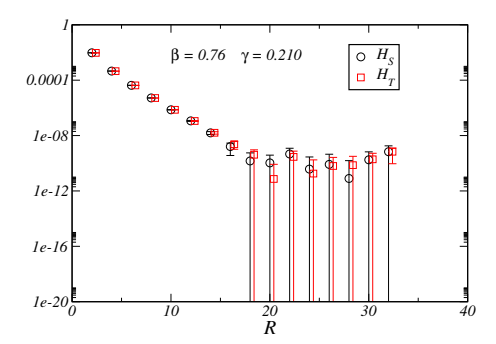


Figure 8: The FM operators in the confinement (left panel) and in the deconfinement (right panel) phase near the confinement to deconfinement transition at  $\gamma = 0.21$  on L = 64 lattice. The critical point is at  $\beta = 0.75314$ . In both panels data for  $H_T$  has been slightly shifted with respect to data for  $H_S$  for clarity, and a logarithmic scale has been used in the vertical axis.

To decrease the variance of the observables we used a "multihit" method [17]. It consists in replacing each link variable in the operator (or the pair of link variables forming each of the corners) with their averages taken by keeping fixed the link

variables which share the same plaquette with them. To decrease the autocorrelation time and avoid the simulation trajectory getting "stuck" around a local energy minimum, a cluster update [18] for the Higgs fields was employed.

The results of simulations are shown in Figs. 6, 7, 8. In all cases data are shown for R even and from R=2 to R=L/2. The left panel of Fig.6 presents the behavior of the FM operator in the Higgs phase above the critical point on a lattice with spatial size L = 64. Clearly, both the spatial and the temporal operators tend to a constant with increasing distance. This constant increases with the value of the Higgs coupling  $\gamma$ , as expected. We have also checked whether there is a volume dependence of the constant. The typical behavior is shown on the right plot of Fig.6, which tells us that the volume dependence of the FM operator is negligible in the Higgs phase. In Fig.7 we show the FM operator at the same gauge coupling  $\beta = 1.0$  for two  $\gamma$  values in the deconfined phase. Deeply in this phase (left panel) the FM operator on the lattice L=64 decreases to a value that is compatible with zero (note the logarithmic scale). The right panel shows the FM operator close to the critical point. Both operators decrease slowly after some large distance and one could conclude that they approach a constant when R is large enough. However, here we have found an essential volume dependence: this constant becomes smaller with increasing volume and might well vanish in the thermodynamic limit. We could not go to larger lattices to check this hypothesis further, but data in Fig.7 strongly support this scenario. Finally, in Fig.8 we have depicted the FM operators in the vicinity of the confinement-deconfinement phase transition for  $\gamma = 0.21$  and two values of the gauge coupling on a L=64 lattice. In both phases the FM operators tend to a small constant compatible with zero. This is expected in the deconfined phase. We can only assume that the constant value in the confinement phase close to the phase transition is very small, so much so that to distinguish it from zero much larger lattices and statistics are required. We have also performed simulations deeply in the confined phase for  $\beta = 0.1, 0.3$ . For all  $\gamma > \beta$  both FM operators approach 1 with distance very fast, while for  $\gamma < \beta$  they rapidly decrease to a very small value.

# 4 Summary

In this paper we studied the Z(2) gauge-Higgs lattice model at finite temperature. Our main goal was to clarify if the Fredenhagen-Marcu operator can be used as an order parameter at finite temperature to distinguish the deconfined phase from the rest of the phase diagram. The crucial point is to prove that the large-distance limit

of the FM operator vanishes in the deconfined phase, while it tends to a constant in the confinement and Higgs phases.

A similar analysis has been done by some of us for the (3+1)-dimensional SU(2) gauge-Higgs LGT in a recent paper [10] where, moreover, a simple non-rigorous argument was advanced to explain why the large distance limit of the FM operator can vanish in the deconfined phase, and its behavior was studied by numerical simulations. The results obtained were, however, not conclusive as larger lattices are needed to get reliable predictions in this model. Therefore, we decided to study the simpler Z(2) LGT, where larger lattice sizes and statistics can be employed without much effort. Our main findings can be briefly summarized as follows.

- We have studied the phase diagram of the Z(2) gauge-Higgs theory by employing local observables like the Polyakov loop, expectation values of the plaquette and Higgs action. This allowed us to locate the critical lines of phase transitions and check the universality class of the model. The collapse plots for the susceptibility of the Polyakov loop show that the model is in the universality class of 2d Ising model. This ensures that the spatial lattice volume is large enough, so the system can indeed be considered as a finite-temperature system.
- The large-distance behavior of both the spatial and temporal FM operators in the deconfined phase seems to be consistent with zero, especially deeply in this phase, *i.e.* at small values of the Higgs coupling. Close to the critical point the FM operators decrease rather slowly with the distance and reach a constant value for the largest distance away from zero. However, this constant decreases with the volume and seems to tend to zero.

The deconfinement phase transition in QCD is associated with a crossover transition at physical quark masses. As we already emphasized, this cannot rule out a non-analytic behavior of some non-local observables. Therefore, as a next step in our investigation of the properties of FM operators, we intend to study its behavior in gauge models coupled with fermions. This can potentially give a direct access to the detection of the deconfinement phase in QCD at finite temperature.

**Acknowledgments**. Authors BA, OB and AP acknowledge support from the INFN/NPQCD project. This work is partially supported by ICSC – Centro Nazionale di Ricerca in High Performance Computing, Big Data and Quantum Computing, funded by European Union – NextGenerationEU. Most numerical simulations have

been performed on the CSN4 cluster of the Scientific Computing Center at INFN-Pisa. VC acknowledges support by the Deutsche Forschungsgemeinschaft (DFG, German Research Foundation) through the CRC-TR 211 'Strong-interaction matter under extreme conditions' – project number 315477589 – TRR 211.

# References

- [1] J. Preskill and L. M. Krauss, Nucl. Phys. B **341** (1990), 50.
- [2] O. Borisenko, M. Faber and G. Zinovjev, Nucl. Phys. (Proc. Suppl.) 63A-C (1998), 409.
- [3] O. Borisenko, M. Faber and G. Zinovjev, "On the deconfinement phase transition in hot gauge theories with dynamical matter fields", hep-lat/9804009.
- [4] K. Fredenhagen and M. Marcu, Phys. Rev. Lett. **56** (1986), 223.
- [5] J. C. A. Barata, Commun. Math. Phys. **129** (1990), 511.
- [6] M. P. Forsström, Electron. J. Probab. **29** (2024), 1.
- [7] T. Filk, M. Marcu and K. Fredenhagen, Phys. Lett. B 169 (1986), 405.
- [8] B. Allés, O. Borisenko and A. Papa, Phys. Rev. D 111 (2025), 014509.
- [9] C. Bonati, G. Cossu, M. D'Elia and A. Di Giacomo, Nucl. Phys. B 828 (2010), 390.
- [10] B. Allés, O. Borisenko and A. Papa, Phys. Rev. D 112 (2025), 094509.
- [11] M. P. Forsström, private communication.
- [12] C. Bonati, A. Pelissetto and E. Vicari, Phys. Rept. 1133 (2025), 1.
- [13] K. Osterwalder and E. Seiler, Annals Phys. 110 (1978), 440.
- [14] E. Fradkin and S. H. Shenker, Phys. Rev. D 19 (1979), 3682.
- [15] J. Greensite and K. Matsuyama, Symmetry 14 (2022), 177.
- [16] A. Ferrenberg and R. Swendsen, Phys. Rev. Lett. 63 (1989), 1195.

- [17] G. Parisi, R. Petronzio and F. Rapuano, Phys. Lett. B 128 (1983), 418.
- [18] R. H. Swendsen and J.-S. Wang, Phys. Rev. Lett. 58 (1987), 86.